

# Performance assessment of solute transport upscaling methods in the context of nuclear waste disposal

E.F. Cassiraga\*, D. Fernández-García, J.J. Gómez-Hernández

*Departamento de Ingeniería Hidráulica y Medio Ambiente, Technical University of Valencia, 46071 Valencia, Spain*

Accepted 2 March 2005

Available online 25 May 2005

## Abstract

Stochastic simulations of solute transport in heterogeneous  $\log_{10}K$  random fields were conducted at two different support scales to assess solute transport upscaling methods in the context of nuclear waste disposal. A very fine grid-scale is used to obtain a reference solution of the real problem, which is based on data from the Sellafield site. A coarse-scale model is obtained by upscaling the heterogeneous grid-blocks onto equivalent homogeneous hydraulic conductivity tensors calculated using the Simple Laplacian Technique. Random fields were designed with different degrees of heterogeneity such that the standard deviation of  $\log_{10}K$  ranged between 0 and 1. It is shown that the early arrival time of particles at a control location, reflected in the lower limit of the 95% confidence interval of the mass flux cumulative density function stochastic process, associated with the upscaled model is strikingly similar to the one associated with the real solution for all heterogeneities. This is encouraging for the application of upscaled stochastic models to the design of nuclear waste repositories where the design of a nuclear waste disposal facility relies on the estimation of the early travel time of radionuclides arriving at a control location. On the contrary, the late arrival time of particles at the control location is largely underestimated by the upscaled model.

© 2005 Elsevier Ltd. All rights reserved.

*Keywords:* Hydrogeology; Groundwater flow; Mass transport; Upscaling; Geostatistics; Stochastic simulations; Nuclear waste disposal

## 1. Introduction

Deep geological repositories are considered as the most feasible and safe solution for the management of radioactive waste. For this reason, the deep disposal of high activity and long live radioactive waste in granite, salt, and clay formations is currently under continuous investigation in many countries of the European Union. In close co-operation on a European level, the EC-funded project BENCHPAR was conceived to study the thermohydromechanical processes occurring in underground radioactive waste repositories. In particular, the BENCHPAR project addressed the problem of upscaling of the thermohydromechanical

parameters proposing several performance assessment exercises in the context of nuclear waste disposal.

The need for upscaling methodologies stems from both the impossibility of modeling physical processes at the scale of measurements and the large spatial variability in dominant parameters [1]. That is, the scales at which measurements are taken are frequently orders of magnitude smaller than the scale at which potential fields for underground waste repositories are discretized for the numerical solution of the conceptual problem. At the same time, parameters such as hydraulic conductivity have been observed in the field to inherit considerable spatial variability. For these two reasons: disparity between measurement scales and computational scales, and spatial heterogeneity, it is necessary to develop upscaling methodologies that permit transforming the information collected at the fine measurement scale into a coarser computational scale well-suited for modeling purposes.

\*Corresponding author. Dep Ingeniería Hidráulica y Medio Ambiente, Universidad Politécnica de Valencia, Camino de Vera s/n, 46071 Valencia, Spain.

*E-mail address:* [efc@hima.upv.es](mailto:efc@hima.upv.es) (E.F. Cassiraga).

This paper presents the work conducted by the Hydrogeology Group at the Technical University of Valencia in which up to date upscaling methodologies were evaluated in the context of the BENCHPAR project [2]. The final objective of the proposed exercise is to compare the actual fate and transport of a fictitious radioactive waste leakage from an underground repository with one simulated at a coarse numerical grid-scale obtained after upscaling. A fine-scale model simulates the real system and is used as a reference solution with which numerical upscaling methodologies will be tested. The exercise simulates a common engineering problem frequently encountered during the design of a deep geological underground repository for the disposal of radioactive wastes. The estimation of radionuclide early arrival time at a control location can make the difference between the acceptance or rejection of a given site. The conceptual problem is parameterised using field data from the Sellafield site UK, but the geometry considered is entirely generic and not specific to any location.

Because thermomechanical processes are only significant at the near field of underground repositories, the large-scale behavior of radioactive waste is mainly controlled by the hydraulic parameters. Among them, because of its large spatial variability, it is widely recognized in the literature that hydraulic conductivity is the dominant parameter controlling the fate and transport of solute transport at large scales [3–5]. Thus, in this work, upscaling methodologies only considered hydraulic conductivity.

It is noted that upscaling implies a simplification in which not all the information on the spatial variability of the parameters can be transferred into the coarser scale. As a consequence, upscaling rules are parameter-specific and goal-oriented techniques. During the upscaling process, it should be decided what is the information that must be transferred between scales. In this respect, the upscaled numerical model for the design of an underground radioactive repository should be able to reproduce the early arrival time of radionuclides at a control location. This is the approach selected in this work, which is conceptually different from other methodologies that focus on the mean arrival time of solute particles [6–9].

The upscaling exercise is based on stochastic simulations that contemplate different equiprobable realizations of a site based on data from the Sellafield site. Parameter values are only sparsely known, thus the multiple realizations are plausible representations of how the site may look like. Each realization is constrained locally by the data values, and globally by the overall statistics imposed on each realization, i.e., mean, variance, or correlation function.

Each realization is generated at the smallest scale, in a real case, this scale should correspond to that at which

the data had been taken, and it is then subjected to an upscaling process. Groundwater flow and mass transport were modeled in both the fine-scale model and in the upscaled model. Then, both solutions are contrasted in order to establish the upscaling rules that provide an upscaled model that captures those aspects of the fine-scale simulation relevant to the problem at hand.

The organization of the paper is as follows: Section 2 describes the properties and geometry of the conceptual model at the fine-scale; Section 3 explains the generation of the hydraulic conductivity random fields at the fine-scale. Sections 4 and 5 describe the flow and transport problems. Section 6 defines the selected upscaling methodology for the hydraulic conductivity. Section 7 presents the simulation results. Finally, Section 8 summarizes the main results and conclusions.

## 2. Conceptual model: based on the Sellafield data

The conceptual model at the fine-scale is a two-dimensional vertical cross-sectional model. Its geometry and main characteristics are depicted in Fig. 1. The size of the domain is 5000 m in the  $x$ -direction and 1000 m in the  $y$ -direction. Groundwater flow is driven by topography from the recharge area to the sea. The model comprises four geological formations with different hydraulic properties. Two horizontal geological formations 500 m thick and one major vertical fracture 5 m wide are distinguished. Hydraulic properties of the portion of the fracture associated with the first and second formations are different. An underground radioactive repository 100 m-wide and 10 m-high was situated 20 m below the top of the lowest formation. The hydraulic conductivity tensor at the fine-scale is assumed to be isotropic.

The hydraulic properties are assumed such that the base 10 logarithm of hydraulic conductivity for each geological formation follows a multi-Gaussian distribution. Table 1 presents the mean and standard deviation of the  $\log_{10} K$  for each geological formation.

The conceptual model was discretized in square cells of 5 m  $\times$  5 m, providing a total of 1000  $\times$  200 grid-cells. Each cell is assigned a hydraulic conductivity value generated stochastically as detailed in Section 3. Each realization generated at the fine-scale model will be used as a reference to test upscaling methodologies.

## 3. Generation of hydraulic conductivity random fields

Hydraulic properties presented in Table 1 were modified for the following two reasons: (i) to emphasize the impact of the vertical fracture in the model by increasing its conductivity, therefore accentuating the difference in hydraulic conductivity between the fracture

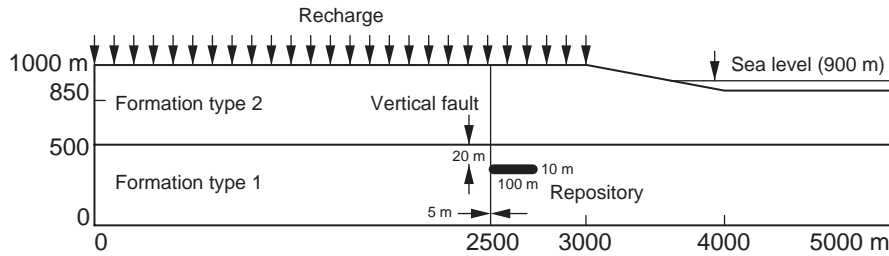


Fig. 1. Schematic of the conceptual model of the Sellafield site.

Table 1  
Hydrogeological properties of the conceptual site

Formation type	Mean of $\log_{10} K$	Standard deviation of $\log_{10} K$
Formation 1	-10.246	0.48
Formation 2	-6.07	0.604
Fracture in formation 1	-10.343	0.865
Fracture in formation 2	-5.57	0.604

Table 2  
Statistical properties of the formations used in simulations

Formation type	Mean of $\log_{10} K$	Standard deviation of $\log_{10} K$
Formation 1	-10.246	0.0, 0.2, 0.4, 0.6, 0.8, 1.0
Formation 2	-6.07	0.0, 0.2, 0.4, 0.6, 0.8, 1.0
Fracture in formation 1	-6.343	0.0, 0.2, 0.4, 0.6, 0.8, 1.0
Fracture in formation 2	-3.57	0.0, 0.2, 0.4, 0.6, 0.8, 1.0

and the adjacent geological formation; and (ii) to analyze how sensitive are the simulation results for various levels of heterogeneity. To achieve this, the mean  $\log_{10} K$  for the fracture in formation 1 was increased from -10.343 to -6.343, and the mean  $\log_{10} K$  for the fracture in formation 2 was increased from -5.57 to -3.57. Six different standard deviations of  $\log_{10} K$  ranging from 0 to 1 were considered in generating random hydraulic conductivity fields (0.0, 0.2, 0.4, 0.6, 0.8, and 1.0). These parameters are presented in Table 2.

Because the conceptual model consists of four different geological formations, each realization at the fine-scale was obtained by assembling four different non-conditional multi-Gaussian random fields each with the mean and variance of the corresponding formation. The generation was performed using the sequential simulation code, GCOSIM3D [10]. Exponential variograms with a nugget equal to 10% of the variance, and a sill equal to the variance were used to generate the random fields. The principal axes of anisotropy were aligned with the Cartesian axes. The patterns of heterogeneity imposed to the realizations were based on scattered information from short interval pumping tests that suggested a correlation of few tens of meters and discussion with experts familiar with the data. Although it appears that most of the fracturing is subvertical showing a strong anisotropy of about 1/5, the anisotropy ratio used during simulations was reduced to 1/2 after testing larger anisotropy ratios, which resulted in unrealistic flow and transport behavior of the model. The range in the  $x$ -direction was equal to 10 m and the range in the  $y$ -direction was equal to 20 m.

Stochastic simulations involved 100 realizations of hydraulic conductivity fields for each  $\log_{10} K$  standard deviation considered. In total, six groups of 100 realizations each with properties provided in Table 2 were generated. These  $\log_{10} K$  random fields were used as input in the groundwater code to solve for piezometric heads and interface flow rates, and then for mass transport modeling by particle tracking.

#### 4. Description of the groundwater flow problem

Under steady-state flow conditions, the partial differential equation of groundwater flow is written as [11]

$$\sum_{i=1}^3 \sum_{j=1}^3 \frac{\partial}{\partial x_i} \left( K_{ij}(\vec{x}) \frac{\partial h(\vec{x})}{\partial x_j} \right) + W(\vec{x}) = 0, \quad (1)$$

where  $h$  is the piezometric head,  $K_{ij}$  is the hydraulic conductivity tensor, and  $W$  is the source/sink term. A 7-point finite difference groundwater flow code, MODFLOW [12], was used to solve the flow Eq. (1). The generated hydraulic conductivity random fields were used as input parameters. Recharge was included through the source/sink term. Boundary conditions were no-flux at the bottom and at both sides of the model. To simulate that groundwater flow is driven by topography from the recharge area to the sea, piezometric heads were set equal to 150 m in grid-cells situated in the recharge area at the top of the model, while piezometric heads in grid-cells located where the sea were set equal to 100 m. Prescribed piezometric

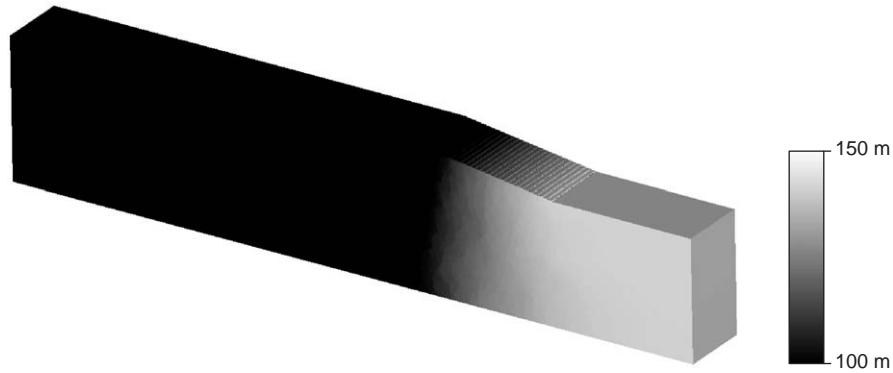


Fig. 2. Stack of the ensemble of 100 piezometric head random fields obtained solving the flow problem for 100 different realizations of the fine-scale hydraulic conductivity random field with standard deviation of  $\log_{10} K$  equal to 1.0.

heads for the portion of the top of the model between the recharge area and the sea, varied linearly from 150 m ( $x = 3000$  m) to 100 m ( $x = 4000$  m). The flow problem was solved at steady state with the mentioned boundary conditions. Fig. 2 shows the ensemble of piezometric head random fields obtained solving the flow problem for 100 different realizations of the hydraulic conductivity random field with standard deviation of  $\log_{10} K$  equal to 1.0.

## 5. Description of the solute transport problem

Under steady-state flow conditions, non-reactive solute transport through heterogeneous porous media is governed by the following differential equation [11,13]:

$$\phi \frac{\partial C(\vec{x}, t)}{\partial t} = - \sum_{i=1}^3 q_i(\vec{x}) \frac{\partial C(\vec{x}, t)}{\partial x_i} + \sum_{i=1}^3 \sum_{j=1}^3 \frac{\partial}{\partial x_i} \left( \phi D_{ij}(\vec{x}) \frac{\partial C(\vec{x}, t)}{\partial x_j} \right), \quad (2)$$

where  $C$  is the dissolved concentration of solute in the groundwater,  $\phi$  is the porosity,  $D_{ij}$  is the dispersion tensor, and  $q_i$  is the  $i$ th-component of Darcy's velocity defined as

$$q_i(\vec{x}) = - \sum_{j=1}^2 K_{ij}(\vec{x}) \frac{\partial h(\vec{x})}{\partial x_j}. \quad (3)$$

In this paper, solute transport was simulated by pure advection (i.e.,  $D_{ij}$  was neglected), in which solute mass, assumed to be inert, is carried by the groundwater flow. It is assumed that the dispersion of solute in the system is mainly due to the heterogeneity of the hydraulic conductivity field. This is a reasonable approximation in most field situations where the advective transport term is much larger than the dispersive term and for those

engineering problems in which the interest lies on the large-scale behavior is the parameter. The selected transport solver was a particle tracking code similar to the one by Ref. [14]. The solute mass is partitioned into particles, each particle representing a portion of the total mass. The motion of a non-reactive solute mass particle in a velocity field is governed by the following kinematical integral equations:

$$X_{p,i}(t + \Delta t) = X_{p,i}(t) + \int_t^{t+\Delta t} V_i(X_{p,1}(\tau), X_{p,2}(\tau)) d\tau, \quad (4)$$

where  $X_{p,i(t)}$  is the  $i$ th-component of the particle location vector at time  $t$ ,  $V_i$  is the  $i$ th-component of the velocity vector at the particle position, and  $\Delta t$  is the elapsed time from the release of the solute. The solution of Eq. (4) requires knowing the velocity field at every point in the system. Because the groundwater flow model, MODFLOW, only provides interface velocities, an interpolation scheme must be selected to obtain a velocity field. A linear interpolation scheme was selected such that the  $i$ th-component of the velocity of a particle moving within a numerical grid-cell was calculated as a linear interpolation between the two face velocities of the grid-cell in the  $i$ -direction. This scheme ensures preservation of mass. The integral in the right hand side of Eq. (4) was solved using Euler's method. A constant displacement scheme [14] was used to move the particles in the domain by which the particles were ensured to take at least 20 displacements steps within a grid-cell. One hundred particles were uniformly distributed along the floor of the repository simulating a uniform radioactive spill. The model describes in detail the movements of the particles generating the following information: velocity vector at the particle position as a function of travel time, travel time of particles crossing the control location

(in this case determined by the sea bed), particle paths, number of displacements and travel distance for each particle, and others. The probability density function of mass flux passing through the control location is the mass flux breakthrough curve obtained at the control location [9]. Fig. 3 illustrates the histogram of the ensemble of particle travel times obtained at the control location (the sea bed) for different standard deviations of the  $\log_{10} K$ .

### 6. Upscaling methodology

Each realization of the hydraulic conductivity field for the Sellafield site was upscaled to a coarser grid-block discretization. An upscaling procedure was applied over square regions of the fine-scale model, which yielded a total of 100 by 20 square grid-blocks of 50 m side (each upscaled block contains 10 by 10 fine-scale grid cells). The upscaling methodology used in this paper is known

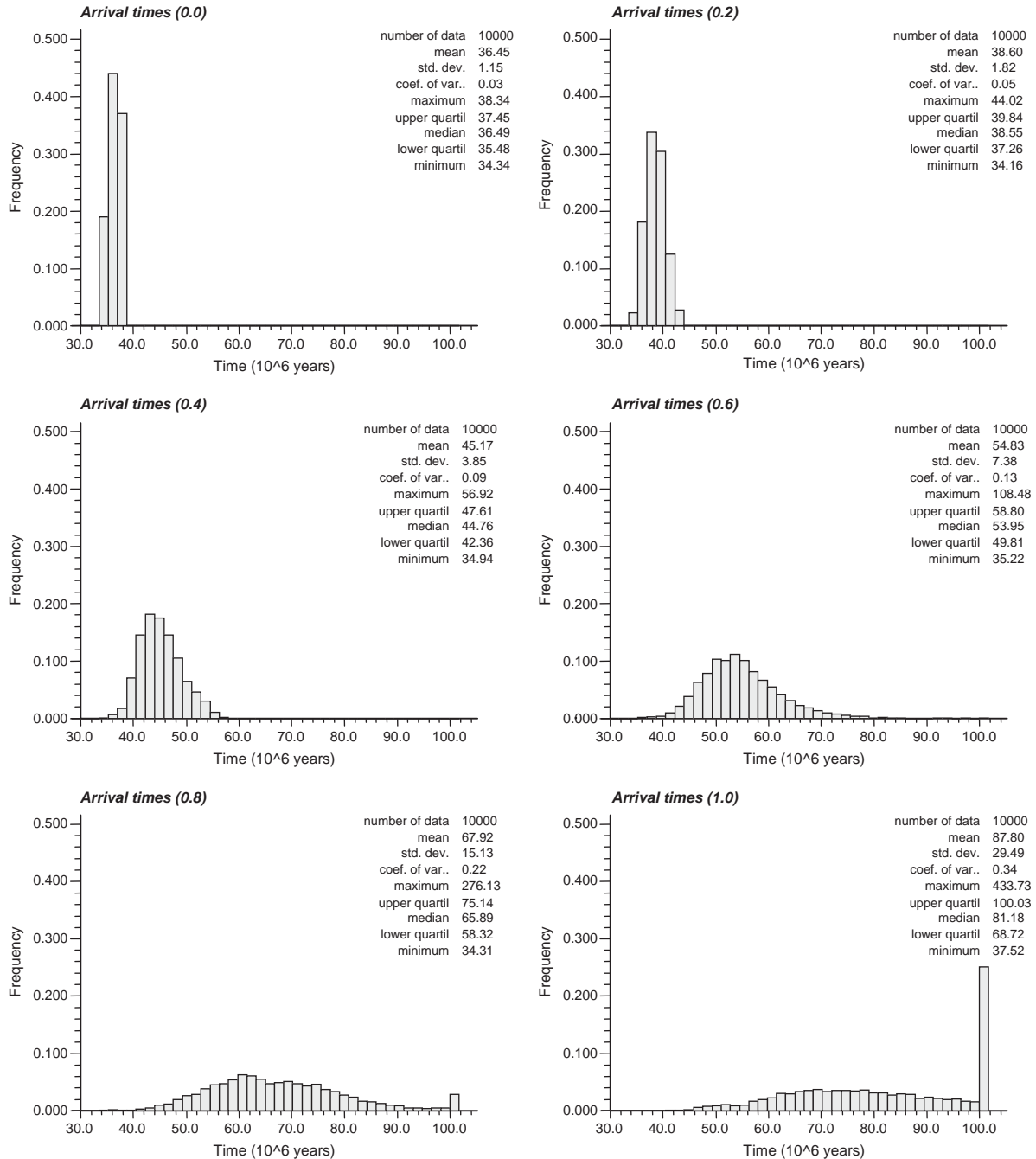


Fig. 3. Histogram of the ensemble of particle travel times obtained at the control location (the sea bed) for different standard deviations of the  $\log_{10} K$  (0.0, 0.2, 0.4, 0.6, 0.8, 1.0).

in the literature as the Simple Laplacian Technique [1,15–17].

The region being upscaled is isolated from the rest of the system. The principal components of the block conductivity tensor are assumed parallel to the block sides (the  $x$  and  $y$ -direction in this case), and each principal component is computed by numerically solving the flow problem with prescribed heads at the faces of the block transverse to the principal direction and impermeable otherwise. In two dimensions, this amounts to solving the flow problem twice for each grid-block.

The expression used to calculate the upscaled grid-block hydraulic conductivity tensor can be written as [1]

$$\{K_V\} = \begin{bmatrix} K_{xx} & 0 \\ 0 & K_{yy} \end{bmatrix} = \begin{bmatrix} Q_x J_x / A_x & 0 \\ 0 & Q_y J_y / A_y \end{bmatrix}, \quad (5)$$

where  $Q_i$  is the total flow flux across the cross-sectional area  $A_i$  transverse to the mean flow direction, the subscript  $i$  denotes the direction of the mean flow, and  $J_i$  is the mean hydraulic gradient for the  $i$ -direction.

After upscaling the fine-scale hydraulic conductivity random field, new  $\log_{10} K$  random fields were obtained at a coarser scale. These upscaled  $\log_{10} K$  random fields were also used as input for solving the flow and transport problems in Eqs. (1) and (4), and ultimately gave the upscaled model solution. Fig. 4 shows the ensemble of piezometric head random fields obtained by solving the flow problem for 100 different realizations of the upscaled hydraulic conductivity random field with standard deviation of  $\log_{10} K$  equal to 1.0.

## 7. Simulation results

Simulation results are presented in Fig. 5, where the mass flux cumulative distribution function (cdf) obtained using the upscaled model are contrasted with those associated with the real system obtained using the fine-scale model. The slope of the mass flux cdf

determined at the travel time at which 50% of the injected mass passed the control plane quantifies “macrodispersion”, which solely originated by heterogeneity in  $\log_{10} K$  in this case. The smaller the angle of the slope, the more solute dispersion occurs in the system due to heterogeneity in  $\log_{10} K$ . Fig. 5 illustrates that macrodispersion is directly related to the degree of heterogeneity measured by the standard deviation of  $\log_{10} K$ . As expected, macrodispersion increases with heterogeneity such that the slope of the mass flux cdf for the real system decreases with the standard deviation of  $\log_{10} K$ . This is in agreement with field observations [18] and with stochastic theories on solute transport [3,5].

However, this effect of increasing macrodispersion with heterogeneity is less significant for the upscaled model in comparison with the real system. In the upscaling process, important fine-scale information is suppressed; the spatial variability of hydraulic conductivity in a grid-block is replaced by an equivalent homogeneous medium, therefore, losing crucial information on the preferential paths that a solute particle may favor within the grid-block. As a consequence, upscaled simulations exhibited mass flux cdfs steeper than those attributed to the real system (fine-scale simulations). In addition, the 50% travel time of particles  $t_{50}$ , defined as the travel time at which 50% of the mass has passed through the control plane, for the upscaled model are smaller than those attributed to the real system at the fine-scale. It is noted that uncertainty associated with the mass flux cdfs at the control plane increases with the degree of heterogeneity. This is manifested in Fig. 5 noting that the difference in travel time between the upper limit of the 95% confidence interval of the mass flux cdf stochastic process and the lower limit of the 95% confidence interval of the mass flux cdf stochastic process increases with the standard deviation of the  $\log_{10} K$ .

The design of a nuclear waste disposal facility is mainly based on an estimate of the early arrival time of radionuclides at a control location defined for the

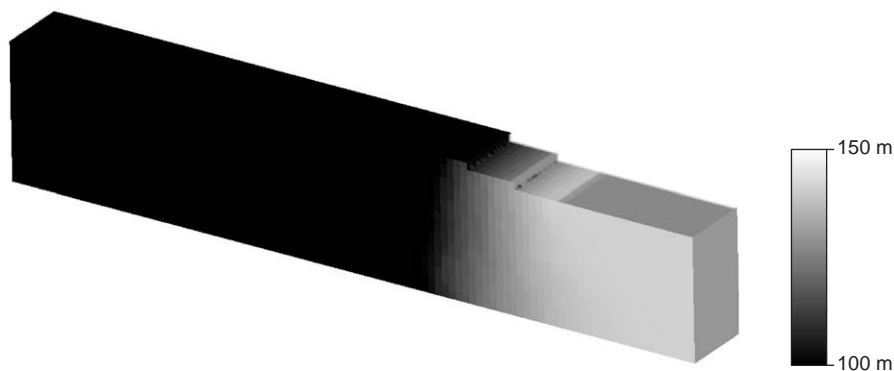


Fig. 4. Stack of the ensemble of 100 piezometric head random fields obtained after solving the flow problem for 100 different realizations of the upscaled hydraulic conductivity random field with standard deviation of  $\log_{10} K$  equal to 1.0.

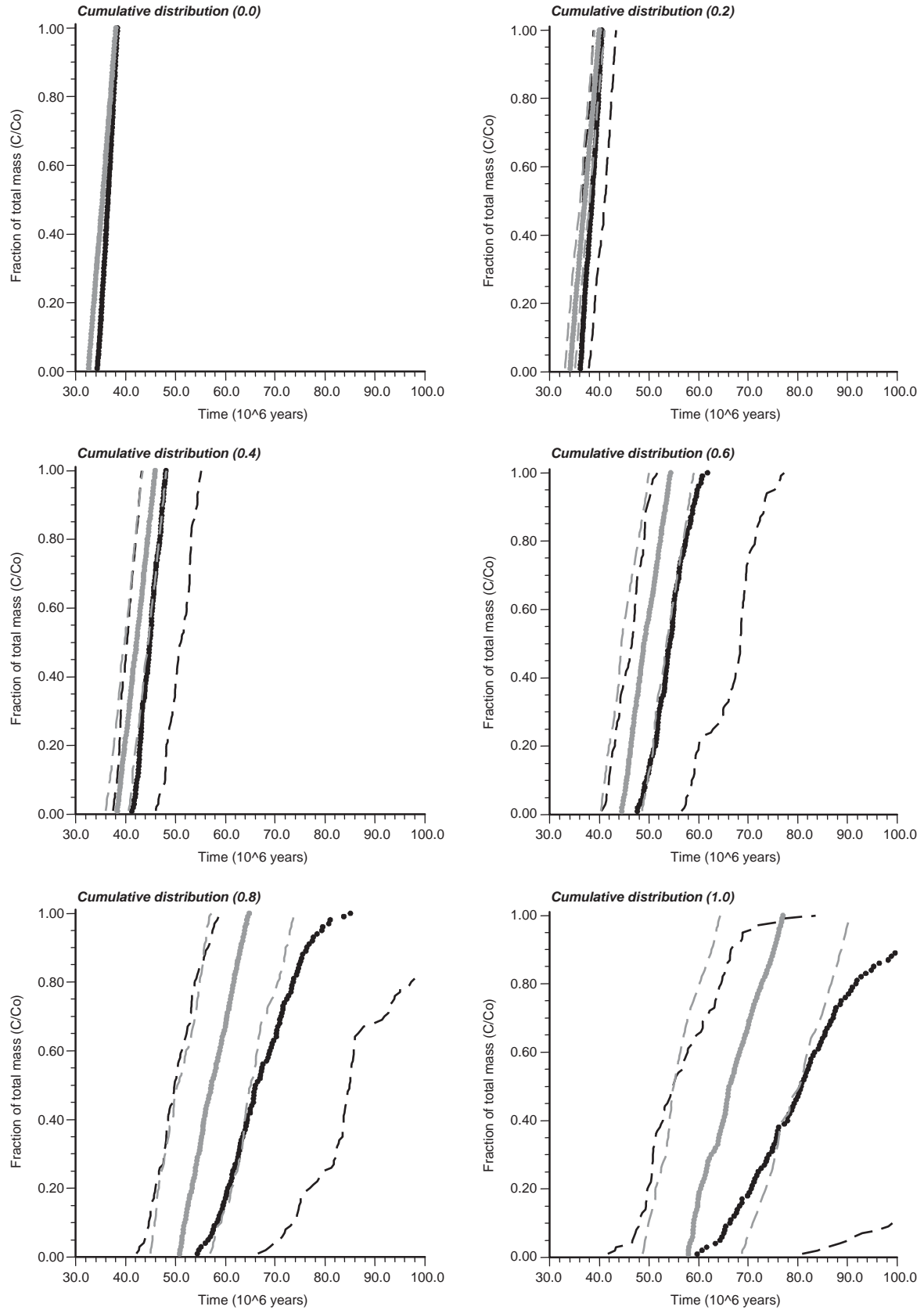


Fig. 5. Ensemble of the cumulative distribution of particle travel times obtained at the control location (the sea bed) for different standard deviations of the  $\log_{10} K$  (0.0, 0.2, 0.4, 0.6, 0.8, 1.0).

protection of the public health or the preservation of the environmental quality. In this context, it should be noted in Fig. 5 that early particle arrival times obtained from both the upscaled model and the real system are remarkably similar. That is, the lower limit of the 95% confidence interval of the mass flux cdf stochastic process for the upscaled model is very similar to the one attributed to the real system (fine-scale). On the contrary, the upper limit of the 95% confidence interval of the mass flux cdf stochastic process for the real system is larger than the one associated with the upscaled model, such that the discrepancy between the fine-scale model and the upscaled model increases with heterogeneity. In practice, these results indicate that stochastic simulations of solute transport at this generic site conducted at the coarse-scale will provide reasonably good estimates of the true early particle arrival times but will largely underestimate the potential late travel time of a particle.

It is also noted from Fig. 5 that the average behavior is not well reproduced in the upscaled model. This discrepancy increases with heterogeneity. We can distinguish two effects: (i) the ensemble average mass flux cdf for the upscaled model is retarded with respect to the real solution, and (ii) the ensemble average mass flux cdf for the upscaled model reflects smaller macro-dispersion coefficients than the real solution. Thus, it appears that in order to match the ensemble average mass flux cdf with the real solution the upscaled model requires both a fictitious retardation factor and a dispersion coefficient. For instance, the fictitious retardation factor can be estimated as the ratio of the mean travel time for the upscaled model to the mean travel time for the real solution. This gives retardation factors ranging from 1.0 for the homogeneous case (standard deviation of  $\log_{10} K$  equal to 0) to 1.2 for the heterogeneous case with standard deviation of  $\log_{10} K$  equal to 1.0.

## 8. Summary and conclusions

We have conducted stochastic simulations of solute transport in heterogeneous  $\log_{10} K$  random fields at two different support scales. The fine grid-scale is used as a reference solution of the real problem, which is based on data from the Sellafield site. The coarse-scale is the upscaled model obtained replacing heterogeneous grid-blocks by equivalent homogeneous hydraulic conductivity tensors obtained using the Simple Laplacian Technique. Random fields were designed with different degrees of heterogeneity such that the standard deviation of  $\log_{10} K$  ranged between 0 and 1. By doing this, we performed an assessment of the solute transport upscaling methods in the context of the nuclear waste disposal. It is shown that the early arrival time of

radionuclide particles, reflected in the lower limit of the 95% confidence interval of the mass flux cdf stochastic process, for the upscaled model is strikingly similar to the one associated with the real solution for all heterogeneities. This is encouraging for the application of upscaled stochastic models to the design of nuclear waste repositories where, in general, the design of a nuclear waste disposal facility is based on the estimation of the early travel time of radionuclide arriving at a control location defined for the protection of public health or the preservation of the environmental quality. On the contrary, the late arrival time of particles at the control location is largely underestimated by the upscaled model. This situation is important in the application of remediation techniques where the running time requisite to recover a certain amount of contaminant mass from the aquifer is the parameter to optimize.

Moreover, comparing the ensemble average mass flux cdf for the upscaled model with the one for the real solution, it is seen that the upscaled model needs to incorporate both a fictitious retardation factor and a dispersion coefficient in order to reproduce the real ensemble average solution.

As expected, it is found that because the upscaling process partially suppressed fine-scale information, the upscaled hydraulic conductivity random field is less heterogeneous. Consequently, the uncertainty associated with the predictions of mass flux in the upscaled model are found smaller than those attributed to the real fine-scale field, such that the confidence interval of the particle arrival time will be largely underestimate by the upscaled model.

## Acknowledgements

Financial aids from the EC through contract FIKW-CT2000-00066 and from the Spanish Nuclear Waste Management Agency, ENRESA, through contract 0770140 are gratefully acknowledged. The third author wishes to thank also the Spanish Ministry of Science and Technology through contract REN2002-02428.

## References

- [1] Gómez-Hernández JJ. A stochastic approach to the simulation of block conductivity fields conditioned upon data measured at a smaller scale. Ph.D. thesis, Stanford University, USA, 1991. 351pp.
- [2] Gómez-Hernández JJ, Cassiraga EF. Impact of flow and transport coupling in the upscaling of transport parameters for performance assessment in the context of nuclear waste disposal. In: Stephansson S, et al., editors. Coupled thermo-hydro-mechanical-chemical processes in geo-systems. Fundamentals, modelling, experiments and applications, Elsevier geo-engineering book series, vol. 2. Amsterdam: Elsevier; 2004. p. 243–50.



- [3] Dagan G. Flow and transport in porous formations. Berlin: Springer; 1989 (461pp).
- [4] Freeze RA. A stochastic-conceptual analysis of one-dimensional groundwater flow in nonuniform homogeneous media. *Water Resour Res* 1975;11(5):725–41.
- [5] Gelhar LW. Stochastic subsurface hydrology. Englewood Cliffs, NJ: Prentice-Hall; 1993 (390pp).
- [6] Dagan G, Cvetkovic V, Shapiro A. A solute flux approach to transport in heterogeneous formations. 1. The general framework. *Water Resour Res* 1992;28(5):1369–76.
- [7] Cvetkovic V, Dagan G, Cheng H. Contaminant transport in aquifers with spatially variable hydraulic conductivity and sorption properties. *Proc R Soc London A* 1998;454:1–36.
- [8] Fernández-García D, Illangasekare TH, Harihar Rajaram R. Conservative and sorptive forced-gradient and uniform flow tracer tests in a three-dimensional laboratory test aquifer. *Water Resour Res* 2004;40:W10103.
- [9] Shapiro AM, Cvetkovic VD. Stochastic analysis of solute arrival time in heterogeneous porous media. *Water Resour Res* 1988; 24(10):1711–8.
- [10] Gómez-Hernández JJ, Journel AG. Joint simulation of multi-Gaussian random variables. In: Soares A, editor. *Geostatistics Tróia'92*, vol. 1. Dordrecht: Kluwer; 1993. p. 85–94.
- [11] Bear J. Dynamics of fluids in porous media. Mineola, NY: Dover; 1972.
- [12] McDonald M, Harbaugh A. A modular three-dimensional finite difference ground-water flow model. US Geological Survey, Open-file Report 1984:83–875.
- [13] Freeze RA, Cherry JA. Groundwater. Englewood Cliffs, NJ: Prentice-Hall; 1979.
- [14] Wen X-H, Gómez-Hernández JJ. The constant displacement scheme for tracking particles in heterogeneous aquifers. *Ground Water* 1996;34(1):135–42.
- [15] Sánchez-Vila X, Girardi JP, Carrera J. A synthesis of approaches to upscaling of hydraulic conductivity. *Water Resour Res* 1995;31(4):867–82.
- [16] Warren JE, Price HH. Flow in heterogeneous porous media. *Soc Petroleum Eng J* 1996;1:153–69.
- [17] Wen X-H, Gómez-Hernández JJ. Upscaling hydraulic conductivities in heterogeneous media: an overview. *J Hydrol* 1996; 183:ix–xxxii.
- [18] Gelhar LW, Welty C, Rehfeldt K. A critical review of data on field-scale dispersion aquifers. *Water Resour Res* 1992;28(7): 1955–74.